doi:10.1016/j.jmb.2003.09.079 J. Mol. Biol. (2003) 334, 403–419

JMB

Available online at www.sciencedirect.com

SCIENCE DIRECT®

ELSEVIER

Nucleotide Dependent Monomer/Dimer Equilibrium of OpuAA, the Nucleotide-binding Protein of the Osmotically Regulated ABC Transporter OpuA from *Bacillus subtilis*

Carsten Horn[1], Erhard Bremer[2] and Lutz Schmitt[1]*

[1]*Institute of Biochemistry Biocenter N210 Johann-Wolfgang Goethe University Frankfurt Marie-Curie Str. 9, 60439 Frankfurt, Germany*

[2]*Laboratory for Microbiology Department of Biology Philipps University Marburg Karl-von-Frisch Str., 35032 Marburg, Germany*

**Corresponding author*

The OpuA system of *Bacillus subtilis* is a member of the substrate-binding-protein-dependent ABC transporter superfamily and serves for the uptake of the compatible solute glycine betaine under hyperosmotic growth conditions. Here, we have characterized the nucleotide-binding protein (OpuAA) of the *B. subtilis* OpuA transporter *in vitro*. OpuAA was over-expressed heterologously in *Escherichia coli* as a hexahistidine tag fusion protein and purified to homogeneity by affinity and size exclusion chromatography (SEC). Dynamic monomer/dimer equilibrium was observed for OpuAA, and the K_D value was determined to be 6 μM. Under high ionic strength assay conditions, the monomer/dimer interconversion was diminished, which enabled separation of both species by SEC and separate analysis of both monomeric and dimeric OpuAA. In the presence of 1 M NaCl, monomeric OpuAA showed a basal ATPase activity ($K_M = 0.45$ mM; $k_2 = 2.3\ min^{-1}$), whereas dimeric OpuAA showed little ATPase activity under this condition. The addition of nucleotides influenced the monomer/dimer ratio of OpuAA, demonstrating different oligomeric states during its catalytic cycle. The monomer was the preferred species under post-hydrolysis conditions (e.g. ADP/Mg^{2+}), whereas the dimer dominated the nucleotide-free and ATP-bound states. The affinity and stoichiometry of monomeric or dimeric OpuAA/ATP complexes were determined by means of the fluorescent ATP-analog TNP–ATP. One molecule of TNP–ATP was bound in the monomeric state and two TNP–ATP molecules were detected in the dimeric state of OpuAA. Binding of TNP–ADP/Mg^{2+} to dimeric OpuAA induced a conformational change that led to the decay of the dimer. On the basis of our data, we propose a model that couples changes in the oligomeric state of OpuAA with ATP hydrolysis.

Keywords: ABC transporter; nucleotide-binding protein; ATPase; monomer/dimer equilibrium; TNP–ATP

Supplementary data associated with this article can be found at doi = 10.1016/j.jmb.2003.09.079

Abbreviations used: AMP-PNP, adenosine 5′-(β-γ imido)-triphosphate; ADP, adenosine diphosphate; ATP, adenosine triphosphate; ABC, ATP-binding cassette; *B. subtilis*, *Bacillus subtilis*; cps, counts per second; CFTR, cystic fibrosis transmembrane conductance regulator; K_D, dissociation constant; γ, enhancement factor; *E. coli*, *Escherichia coli*; GB, glycine betaine; IMAC, immobilized metal-ion affinity chromatography; LDH, lactate dehydrogenase; *L. lactis*, *Lactococcus lactis*; MWCO, molecular weight cut off; M/D, monomer/dimer; NADH, nicotine adenine dinucleotide reduced form; NBD, nucleotide-binding domain; Opu, osmoprotectant uptake; PK, pyruvate kinase; *S. typhimurium*, *Salmonella typhimurium*; SEC, size exclusion chromatography; SBP, substrate-binding protein; TMD, transmembrane domain; TNP, trinitro phenyl; v/v, volume per volume; w/v, weight per volume.

E-mail address of the corresponding author: lschmitt@em.uni-frankfurt.de

Introduction

Many microorganisms such as the Gram-positive soil bacterium *Bacillus subtilis* (*B. subtilis*) are exposed frequently to drastic and sometimes rapid changes in the availability of water in their natural habitat.[1–3] The concomitant alterations in the osmotic gradient between the osmolarity of the environment and the interior of the cell threatens the bacteria with rupture under hypotonic conditions and dehydration under hypertonic circumstances as water moves passively through the cytoplasmic membrane.[4,5] Studies with the enteric Gram-negative bacteria *Escherichia coli* (*E. coli*) and *Salmonella typhimurium* (*S. typhimurium*) revealed that large amounts of K^+ ions (up to 0.4 M) are rapidly taken up from the environment under high osmolarity growth conditions to counteract the efflux of water from the cell and the resulting reduction in cell turgor.[6–8]

Since the cellular machinery of non-halotolerant bacteria is not adapted to conditions of permanent high ionic strength, these bacteria replace rapidly potassium ions with osmotically active organic osmolytes.[1] These so-called "compatible solutes" are highly congruous with cellular functions, and their high-level accumulation is used by the cell as second line of defense to increase cellular water content and to maintain cell turgor within physiologically acceptable boundaries under hypertonic growth conditions.[9] One of the compatible solutes most widely used by prokaryotic and eukaryotic cells is the trimethylammonium compound *N*,*N*,*N*-trimethyl glycine (glycine betaine (GB)).

B. subtilis possesses five osmoprotectant uptake (Opu) systems for compatible solutes. Three of these are involved in GB import (OpuA, OpuC and OpuD).[10–12] OpuD consists of a single polypeptide and belongs to the BCCT family of secondary transporters; OpuA and OpuC have multiple components and are members of the substrate-binding-protein (SBP)-dependent subfamily of the superfamily of ATP-binding cassette (ABC) transporters. The OpuA system consists of three components: the ATPase OpuAA, the integral membrane protein OpuAB and the extracellular SBP OpuAC. This latter protein binds GB with high affinity and specificity and delivers it to the OpuAA/OpuAB protein complex. To prevent its loss into the growth medium, OpuAC is tethered to the cytoplasmic membrane with a lipid modification at its amino terminus.[13] Transcription of the *opuA* operon is under osmotic control, and the accumulation of GB by *B. subtilis* under hyperosmotic conditions allows growth of the cells over a wide range of environmental salinities.[1,2]

ABC transporters are found in all three kingdoms of life.[14,15] These membrane proteins couple ATP hydrolysis with substrate translocation across biological membranes in a vectorial manner. ABC transporters may serve as import or export machineries of an extremely broad set of non-structurally related compounds ranging from small ions, amino acids, sugars and drugs to peptides and even large proteins. Some human members of the ABC superfamily are accountable for diseases or pathophysiological processes, such as bare lymphocyte syndrome, adrenoleukodystrophy, Stargardt macular dystrophy, Tangier syndrome, virus escape and many more.[16] Other examples of human ABC transporters are P-glycoprotein (MDR1),[17] which is responsible for multidrug resistance in cancer therapy, and the gated chloride channel cystic fibrosis transmembrane contuctance regulator (CFTR).[18] Mutations in the CFTR gene are liable for cystic fibrosis, one of the most common deadly inherited diseases among Caucasians.

As a general blueprint, all ABC transporters consist of two nucleotide-binding domains or subunits (NBDs) and two transmembrane domains or subunits (TMDs).[19] The domain organization within ABC transporters is extremely variable. In most of the eukaryotic ABC transporters all four domains are fused into a single polypeptide chain. In contrast, the TMD and NBD of prokaryotic ABC transporters are normally not fused and are encoded by separate genes. Many prokaryotic ABC transporters possess a fifth subunit, the SBP, which per definition does not belong to the ABC transporter.[20] The SBP is located in the periplasm of Gram-negative bacteria or is anchored in the cytoplasmic membrane by a lipid modification of the amino-terminal Cys residue in Gram-positive bacteria. The SBP binds its ligand(s) selectively and with high affinity and delivers it to the substrate translocation complex embedded in the cytoplasmic membrane; the ligand is then pumped into the cell upon ATP hydrolysis.

Biochemical and genetic studies indicate that the TMDs form a dimer as the functional unit in the translocation pathway.[21] These data are supported by the recently solved structures of the ABC transporters BtuCD[22] and MsbA,[23] although the TMDs of these proteins exhibit a different architecture. The TMDs show limited sequence homology as they interact with the transport substrate. The opposite is true for the NBDs, which energize the transport process and, at least in one case, interact with the substrate.[24] At least three highly conserved motifs are generally found in the NBDs: the Walker A and B motifs[25] and the C loop, also known as "signature motif", which is the hallmark of all ABC transporters (bacterial consensus sequence LSGGQ).[14] The first reported crystal structure of an NBD, HisP, the NBD of the histidine permease, revealed an L-shaped two-domain structure.[26] The catalytic domain adopts an α/β fold similar to the RecA protein or the F_1-ATPase.[25] It contains the Walker A and B motifs which are involved in ATP binding and hydrolysis. The helical or signaling domain harbors the C loop at its periphery.[19]

Only limited information is available for the functional oligomerization status of the NBDs. From a biochemical point of view, a transient

dimer formation during the catalytic cycle has been observed for the NBD of the histidine permease HisP[27] and the mutant NBDs of MJ0796 (E171Q) and MJ1267 (E179Q)[28] and the NBD of Mdl1p.[29] Besides MsbA and BtuCD, several structures of isolated NBDs have been solved such as HisP,[26] MalK,[30] MJ0796 (E171Q),[31,32] MJ1267 (E179Q),[33] TAP1-NBD,[34] HlyB-NBD,[35] GlcV[36] and the ABC-related proteins Rad50[37] and ArsA.[38] All these proteins have been crystallized in different functional states. Nevertheless, a relation between functional and oligomeric state of the NBD has still not been elucidated.

In this study we have characterized OpuAA, the NBD of the osmotically regulated ABC transporter OpuA[11,13] from *B. subtilis*. In addition to the characteristic sequence motifs of NBDs of ABC transporters, it contains a roughly 200 amino acid extension at its carboxy terminus. Sequence comparison revealed a high degree of amino acid sequence identity of the *B. subtilis* OpuAA to OpuAA from *Lactococcus lactis* (*L. lactis*)[39,40] (58% identity) and to ProV, the NBD of the ProU ABC transporter from *E. coli*[41] (50% identity). Here, we have overexpressed heterologously OpuAA in *E. coli* and purified it to homogeneity. We observed a concentration-dependent interconversion of monomeric and dimeric (M/D) OpuAA in the nucleotide-free state. Separate isolation of both the OpuAA monomer and the OpuAA dimer was possible under high ionic strength, since M/D interconversion was slowed under these assay conditions. The monomer showed detectable ATPase activity at high ionic strength, whereas the dimer exhibited only a marginal activity. A dissociation constant (K_D) of 6 μM for the M/D equilibrium was determined at 150 mM NaCl. Addition of nucleotides such as ADP/Mg^{2+} or AMP-PNP/Mg^{2+} (a non-hydrolysable ATP analogue) resulted in a shift of the apparent K_D to higher values. The fluorescent ATP analogue TNP–ATP was used to determine affinity and stoichiometry of monomeric and dimeric OpuAA/ATP complexes, respectively. Two TNP–ATPs per dimeric OpuAA and one TNP-molecule per monomeric OpuAA were bound at 150 mM NaCl. Additionally, TNP–ADP was used as a reporter to sense conformational changes of dimeric OpuAA. Taken together, our data indicated a functional coupling of changes in the oligomeric state of OpuAA with ATP hydrolysis.

Results and Discussion

Purification of OpuAA

OpuAA, the NBD of the osmotically regulated ABC transporter OpuA from *B. subtilis* was overexpressed heterologously using the L(+)-arabinose-inducible expression vector pBAD33 (see Material and Methods) in *E. coli* as an N or C-terminal hexahistidine-tagged fusion protein, which allowed its subsequent purification by immobilized metal-ion affinity chromatography (IMAC). Both proteins were eluted from a Zn^{2+}/IDA column by a linear imidazole gradient (see Material and Methods). Purity after the IMAC step was around 95% as judged by SDS-PAGE (Figure 1) with a yield of approximately 15 mg/l cell culture for both fusion proteins. To obtain homogeneous OpuAA, aggregates were removed by size exclusion chromatography (SEC). Besides a peak at the void volume and a high molecular mass peak (>250 kDa), two protein peaks with apparent masses of 150 kDa and 65 kDa were observed. These peaks corresponded to dimeric (calculated mass: 95.4 kDa) and monomeric (calculated mass: 47.7 kDa) OpuAA. A comparison of the sequence of OpuAA with those of other NBDs revealed that OpuAA contains an additional extension at the carboxy terminus of roughly 200 amino acids.[11] Such an extension is also found in MalK of *S. typhimurium* or *E. coli*, where it is thought to interact with MalT, a specific gene activator of the *mal* operon.[42,43] However, such a gene activator for the *opuA* operon in *B. subtilis* has not yet been identified. The crystal structure of dimeric MalK reveals a more stick-like shape due to this C-terminal regulatory domain,[30] which might serve as an explanation for the apparent higher molecular mass of monomeric or dimeric OpuAA in SEC. Biochemically both hexahistidine-tagged fusion proteins proved to be identical. Therefore, the N-terminal hexahistidine-tagged version of OpuAA was employed in all subsequent experiments.

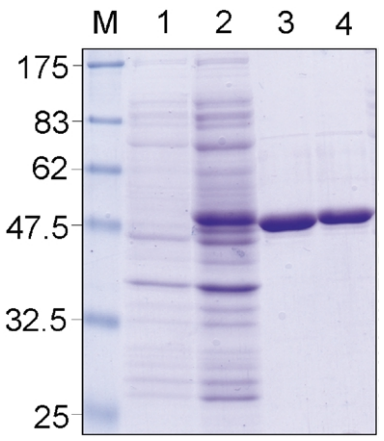

Figure 1. Coomassie-stained SDS-15% PAGE. Lane M, standard molecular masses in kDa; lane 1, total protein of *E. coli* BL21(DE3) harboring pBAD33/OpuAA-His_6 before induction; lane 2, three hours after induction with 0.01% (w/v) L(+)-arabinose; lane 3, 5 μg His_6-OpuAA of pooled elution fractions after IMAC; and lane 4, 5 μg OpuAA-His_6 of pooled elution fractions after IMAC.

Analysis of M/D OpuAA

Purified OpuAA was analyzed in buffer B

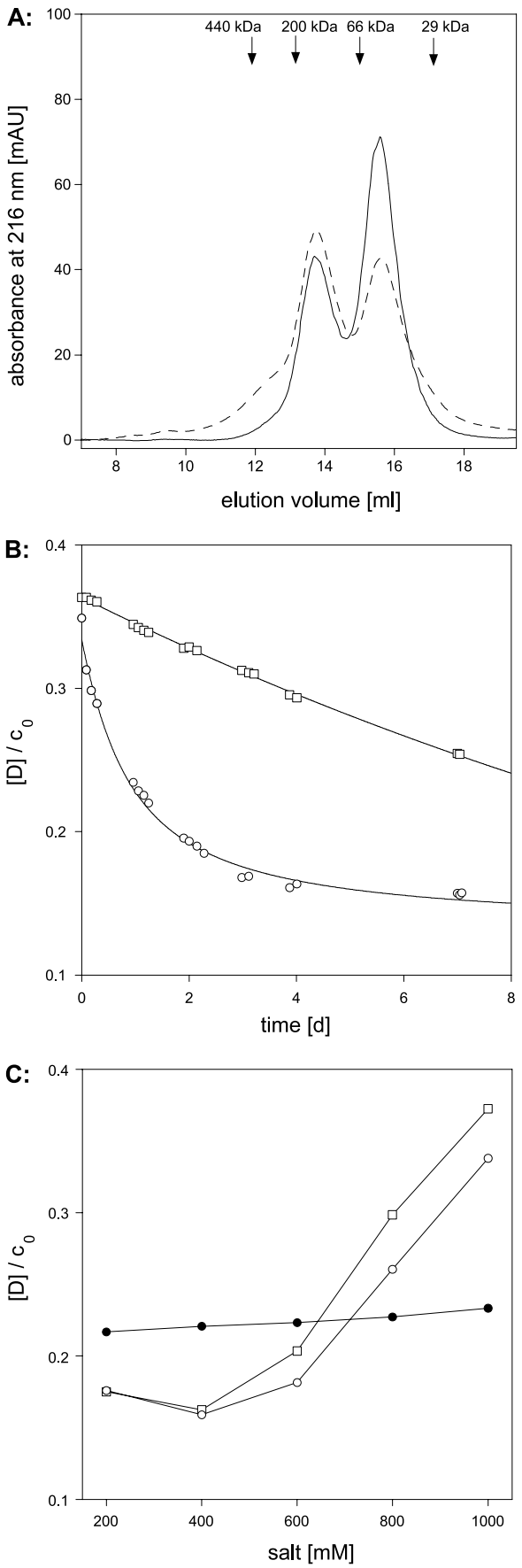

Figure 2. (A) OpuAA was applied onto a Superdex 200 HR column at 2.5 μM (continuous line) or 10 μM (broken line) and protein elution was monitored at 216 nm. Arrows indicate elution volumes of used marker proteins with the corresponding molecular mass. (B) OpuAA was diluted to 3.4 μM in buffer B supplemented with 1 M NaCl (□) or 150 mM NaCl (○) and incubated at 4 °C. Samples were applied onto a Superdex 200 HR column at the indicated time points. The M/D ratio was calculated according to equation (1) and plotted *versus* the time of incubation. The decay was analyzed according to equations (3a) and (3b). (C) OpuAA was diluted to 3 μM in NaCl (□), KCl (○) or GB (●) at the indicated concentrations and incubated for 2 d at 4 °C. Samples were applied to SEC, and the M/D ratio was determined as described in Material and Methods. M/D ratio was plotted *versus* salt concentration of the incubation buffer.

supplemented with 150 mM NaCl by SEC. A change in the monomer/dimer (M/D) peak ratio was observed at two different OpuAA concentrations (Figure 2(A)). The amount of monomeric OpuAA decreased, while the amount of dimeric OpuAA increased with increasing protein concentration. This implied a dynamic M/D interconversion.

To understand this phenomenon in more detail, the time dependence of M/D interconversion was investigated. A concentrated OpuAA sample was diluted into buffer B supplemented with either 150 mM NaCl or 1 M NaCl and stored at 4 °C. The M/D ratio was analyzed after different incubation times by SEC. At 150 mM NaCl, OpuAA showed a dynamic interconversion of both oligomeric species within the experimental time frame (Figure 2(B)). This corresponded to a bimolecular equilibrium reaction. In the early time period (0–12 h) the dimer decayed monoexponentially into monomer, and as the concentration of monomer increased the re-association to the dimer became more dominant. After roughly 4 d the equilibrium value for the M/D ratio was reached and an apparent dissociation constant of $5(\pm 3)$ μM was calculated according to equation (3a). This value is in agreement with the one determined by analyzing the M/D ratio of OpuAA at different concentrations by SEC.

In order to analyze both oligomeric species separately, conditions had to be established that slowed the dynamic M/D interconversion. The energy-providing module OpuAA of the OpuA transporter faces the cytosol, and M/D interconversion might be influenced by changes of cytosolic osmolarity or ionic strength *in vivo*. Indeed, M/D interconversion of OpuAA was influenced by ionic strength *in vitro*. At 1 M NaCl, dimeric OpuAA showed a much slower decay and equilibrium was not reached within the experimental time frame. This decay was fitted by a monoexponential decay function, and a half-time of interconversion $\tau = 16(\pm 0.5)$ d was calculated (Figure 2(B)). In agreement with the OpuAA dimer, the monomer was also stabilized at 1 M

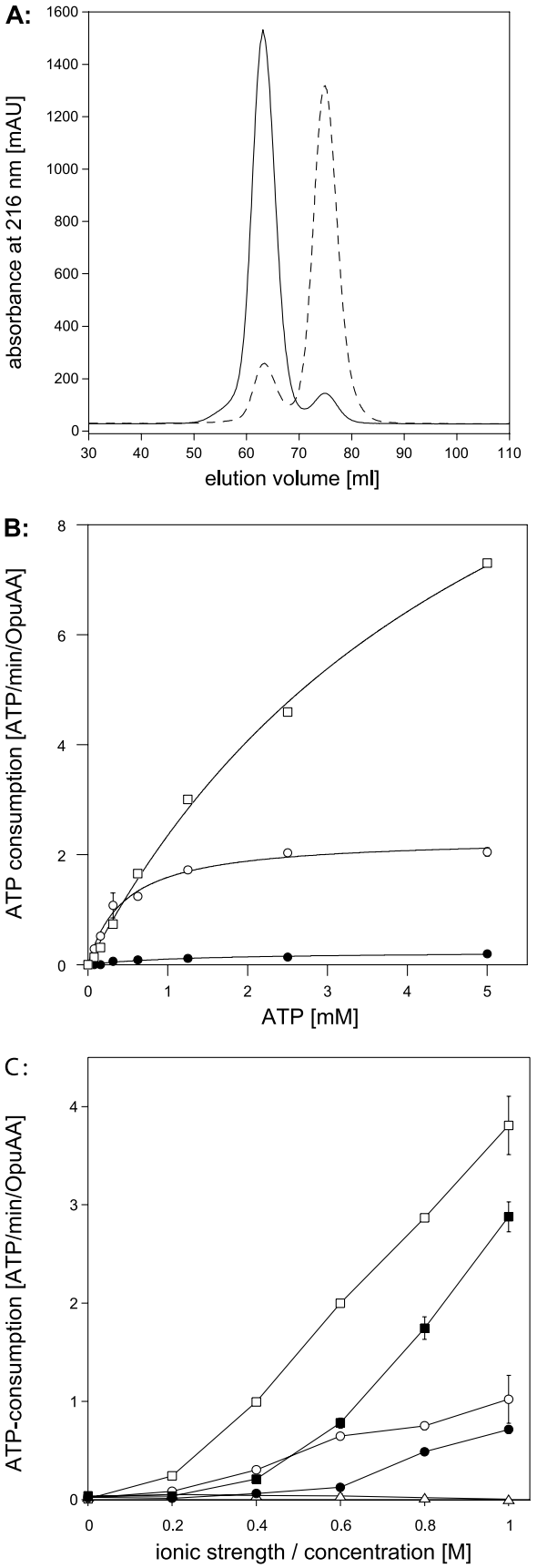

Figure 3. ATPase activity of OpuAA. (A) Monomeric (broken line) and dimeric (continuous line) OpuAA were prepared as described in Results and Discussion and separately applied to a Superdex 200 HR 16/60 SEC column. (B) ATP consumption of monomeric or dimeric OpuAA was analyzed at different ATP concentrations (monomer, 1 M NaCl (○); monomer, 1 M KCl (□); dimer, 1 M NaCl (●)). Reaction velocities were analyzed according to equation (5). (C) ATPase activity of OpuAA M/D was analyzed at 5 mM ATP/Mg^{2+} in KCl (□), KP_i (■), NaCl (○), NaP_i (●), GB (△) at the indicated ionic strength or concentration in the case of GB.

NaCl (data not shown). These observations imply that association and dissociation rates of the M/D equilibrium were slowed at high ionic strength. As a consequence, both oligomeric species could be isolated and analyzed separately at 1 M NaCl.

How does ionic strength or osmolarity influence M/D interconversion? To address this issue, a concentrated OpuAA sample was incubated for 2 d at 4 °C in buffer B supplemented with different salts. To analyze whether the nature of salt had any influence, we analyzed both NaCl and KCl, since the intracellular accumulation of K^+ ions plays an important role in the bacterial defense against hyperosmotic stress.[1] To investigate possible effects of the substrate of the OpuA transporter, GB was also tested. Since GB does not have a net charge at physiological pH, it contributes to osmolarity but not to ionic strength. After a two-day incubation at 4 °C, the M/D ratio was analyzed by SEC. Increasing the salt concentration resulted in an increase in time necessary to reach equilibrium of M/D interconversion (Figure 2(C)). The nature of the cation had hereby no influence. Interestingly, at 0.4 M NaCl or KCl a minimum was observed. In contrast to NaCl or KCl, the compatible solute GB had no influence on the rate of dimer decay over the investigated concentration range. These observations implied that M/D interconversion and equilibrium were influenced by ionic strength but not by osmolarity. This suggests a potential significance of electrostatic interactions in association/dissociation processes of OpuAA. In support of our interpretation, a critical role of subtle balanced electrostatic effects was reported for dimer association of the NBD MJ0796, which contains the E171Q mutation.[28]

Influence of salt on basal ATPase activity

For several isolated NBDs of ABC transporters such as HisP,[27] MalK[44,45] and MJ0796,[28] a basal ATPase activity had been demonstrated. Despite the fact that substrate-stimulated ATPase activity of fully assembled ABC transporters in reconstituted systems is higher than the basal ATPase activity of the isolated NBD,[46] these data might contribute to understand the function and regulation of these domains.

To investigate whether the OpuAA monomer and/or the OpuAA dimer display a basal ATPase activity, both species were isolated separately.

Table 1. Michaelis–Menten parameters of monomeric or dimeric OpuAA at 1 M NaCl or 1 M KCl at 22(± 2) °C

Oligomeric species/salt	K_M (mM)	Turnover number (min^{-1})	Catalytic efficiency ($M^{-1}\,min^{-1}$)
Monomer/1 M KCl	5.4 ± 0.6	15.5 ± 1.10	2900
Monomer/1 M NaCl	0.45 ± 0.06	2.3 ± 0.1	5100
Dimer/1 M NaCl	1.3 ± 0.5	0.24 ± 0.04	190
Monomer and dimer/0.15 M NaCl	0.25 ± 0.1	0.25 ± 0.01	1000

After a first SEC step under high ionic strength, monomer and dimer fractions were pooled separately and applied to a second SEC step in buffer B supplemented with 1 M NaCl or 1 M KCl. Through this purification scheme both species of OpuAA were enriched to more than 90% (Figure 3(A)). ATP consumption of monomeric or dimeric OpuAA was measured at different ATP concentrations in the presence of 1 M NaCl or 1 M KCl. ATP consumption was normalized to the protein concentration and analyzed by standard Michaelis–Menten kinetics (Figure 3(B)). Parameters are summarized in Table 1.

Monomeric OpuAA revealed a basal ATPase activity with a K_M value of 0.45(± 0.06) mM and a turnover number of 2.3(± 0.1) min^{-1} at 1 M NaCl (Table 1). These values are similar to those of other isolated NBDs.[27,44] Testing basal ATPase activity of the monomer in presence of 1 M KCl revealed an increase in both K_M value and turnover number (K_M = 5.4(± 0.6) mM, k_2 = 15.5(± 1.1) min^{-1}). However, the catalytic efficiency of monomeric OpuAA at 1 M NaCl or KCl was similar (Table 1). It is thought that evolutionary pressure increases the K_M value while keeping catalytic efficiency constant.[47] As a first reaction in osmotic stress situations, potassium ions are accumulated to a sub-molar concentration.[1] Therefore, the detected changes might serve as a mechanism to modulate ATPase activity of OpuAA by the interplay of K_M and turnover number; at 1 M KCl, the K_M of the monomer is in the range of the cytosolic ATP concentration, meaning that approximately 50% of the proteins are in the ATP-bound state.

Compared to the monomer, dimeric OpuAA revealed a tenfold lower basal ATPase activity at 1 M NaCl (Table 1). This observation was surprising, since several studies demonstrated that the dimeric NBD was the active oligomeric species. Ames and coworkers measured an exponential increase in ATPase activity of HisP with a linear increment of the protein concentration.[27] This observation suggested a dynamic M/D equilibrium, with the dimer being the active species. Detailed analysis of basal ATPase activity of the NBD MJ0796 revealed cooperative ATP hydrolysis (Hill coefficient for MJ0796 = 1.7[28]). In analogy to HisP, these data propose that the dimer acts as active species in ATP hydrolysis. On the other hand, investigations of the oligomeric state of the nucleotide-free state of NBDs suggested that the monomer is the preferred species. Therefore, a dynamic M/D interconversion between different states of the hydrolysis cycle may be essential for basal ATPase activity. As demonstrated above, this dynamic M/D interconversion of OpuAA was reduced at high ionic strength.

Following another line of argumentation, the interrupted cross-talk between the NBD dimer and the TMDs, which enables substrate translocation in a well-regulated fashion, could disrupt signal(s) from the TMDs, restricting the ATP hydrolysis by the NBD dimer. Preliminary data (unpublished results) indicate that ATPase activity of dimeric OpuAA is restored upon addition of the two other components of the transporter, OpuAB and OpuAC. Alternatively, ATP or ATP/Mg^{2+} binding might be restricted at high ionic strength as described for the HisP dimer.[27]

In the case of the reconstituted OpuA transporter from *L. lactis*, an increase in intravesicular ionic strength stimulated ATPase activity.[48] We compared these observations for the isolated NBD of the *B. subtilis* transporter OpuA. Since OpuAA from *B. subtilis* is a cytosolic protein and interacts with TMDs, it might be exposed directly to alterations of the cytosolic salt environment. In addition, the sequence homology between both transporters implies a conserved mode of action.

Effects of different salts and their ionic strength on the basal ATPase activity of M/D OpuAA were analyzed in presence of 5 mM ATP/Mg^{2+}. As a general observation, basal ATPase activity was stimulated with increasing salt concentrations in a linear fashion. The compatible solute GB had no detectable effect on basal ATPase activity (Figure 3(C)). Interestingly, the nature of the cation (Na^+ or K^+) had a stronger influence on the stimulation of the basal ATPase activity than the nature of the anion (Cl^- or P_i^-). In contrast to our data, Poolman and coworkers observed a stimulating effect of P_i^- salts and acidic phospholipids on the ATPase activity of the OpuA transporter of *L. lactis*.[48] In their model, osmotic stress is transmitted *via* mechanical tension of the membrane, which activates OpuA.[39,48] However, other mechanisms for the osmotical activation of compatible solute transporters have been proposed.[49] Proteins such as ProP[50] from *E. coli* or BetP[51] from *Corneybacterium glutamicum* have C-terminal extensions that are likely to sense ionic strength. Here, we observe a modulation of M/D interconversion and basal ATPase activity of OpuAA by ionic strength. Potassium ions drastically increase the turnover number as well as the K_M value. This

might imply the presence of a K^+-binding site within OpuAA that is activated in hyperosmotic stress situations. Such a K^+ sensor has been identified in the osmoreactive betaine carrier BetP[52] and in the signal kinase KdpD of *E. coli*.[53]

Effect of nucleotides on the M/D ratio

NBDs energize the substrate translocation and thereby undergo different steps in their catalytic cycle: (1) ATP binding, (2) ATP hydrolysis, (3) release of ADP and P_i to enter (4) a nucleotide-free state. The addition of different nucleotides such as AMP-PNP, ATP or ADP to the NBD might be used to mimic these catalytic steps.

OpuAA (4 μM) was maintained in buffer B supplemented with 150 mM NaCl and 10 mM nucleotides in the absence or presence of 10 mM $MgCl_2$ for 4 d at 4 °C. The M/D ratio was determined as described in Material and Methods to analyze the oligomerization state of OpuAA within its catalytic cycle. In the nucleotide-free state, 17(±2) mol% (here, the $[D]/c_0$ ratio is defined as mol%) of dimeric OpuAA was detected with or without $MgCl_2$ (Figure 4(A)). Roughly the same amount of dimeric OpuAA was observed after addition of AMP-PNP (14(±2) mol%). This indicates similar affinities of AMP-PNP to monomeric and dimeric OpuAA, respectively. Incubation with AMP-PNP in the presence of $MgCl_2$ reduced the amount of dimeric OpuAA by about 40%. In the presence of ADP and ADP/Mg^{2+}, the amount of dimeric OpuAA decreased to 3(±0.5) mol% and 1(±0.2) mol%, respectively. As a consequence, monomeric OpuAA was the dominant species under post-hydrolysis conditions (e.g. ADP/Mg^{2+}). When ATP/Mg^{2+} was added to OpuAA the amount of detected dimeric OpuAA was marginal (1(±0.2) mol%). This implies complete hydrolysis of ATP to ADP during the incubation time and represents therefore post-hydrolysis conditions, since the amount of dimeric OpuAA corresponds to the amount detected in presence of ADP/Mg^{2+} but not AMP-PNP/Mg^{2+}.

To quantify the M/D equilibrium of OpuAA within the different steps of the catalytic cycle, the individual K_D values were determined. OpuAA at different concentrations was incubated with 10 mM AMP-PNP/Mg^{2+} or 10 mM ADP/Mg^{2+} or without nucleotide. Protein concentration was determined spectroscopically and by the bicinchoninic acid assay. OpuAA showed a concentration-dependent change of the M/D peak ratio. A K_D value of 6(±1) μM was calculated for the M/D equilibrium of OpuAA in the nucleotide-free state according to equation (2) (Figure 5(B)). The addition of 10 mM AMP-PNP/Mg^{2+} or 10 mM ADP/Mg^{2+} to OpuAA resulted in a shift of the apparent K_D value to 50(±4) μM and more than 200 μM (data not shown), respectively.

For two other NBDs (HisP and MJ0796 (E171Q)) K_D values of the M/D equilibrium in the nucleotide-free state have been determined.[27,28] In

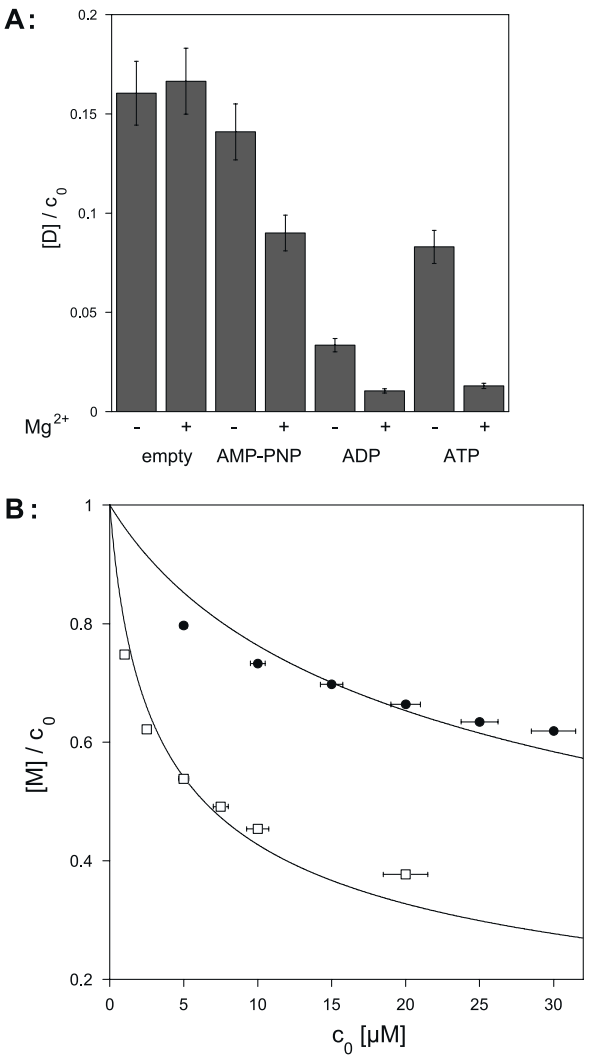

Figure 4. Influence of nucleotides on M/D ratio of OpuAA. (A) 4 μM OpuAA was incubated for 4 d at 4 °C with 10 mM nucleotide in buffer B supplemented with 150 mM NaCl in the absence or presence of 10 mM $MgCl_2$. The M/D ratio was determined as described in Material and Methods. (B) Different concentrations (c_0) of OpuAA were incubated for 4 d at 4 °C without nucleotides (□) or with 10 mM AMP-PNP/Mg^{2+} (●). The M/D ratio was determined as described in Material and Methods and plotted *versus* c_0. The K_D value was analyzed according to equation (2).

contrast to OpuAA, these K_D values are greater by a factor of 15–30 than the one reported here (HisP: 85 μM; MJ0796 (E171Q): 208 μM). Thus for HisP and MJ0796 (E171Q), the monomer is the preferred species for the nucleotide-free state in solution. In contrast, OpuAA formed a stable dimer in the nucleotide-free state even in the absence of the cognate TMDs. In agreement with our data, a dimerization of MalK was demonstrated and proposed as intial step in the assembly of the maltose transport complex.[54]

In the mutant NBDs MJ0796 (E171Q), MJ1267 (E179Q)[28] and Mdl1p (E599Q)[29] a highly conserved

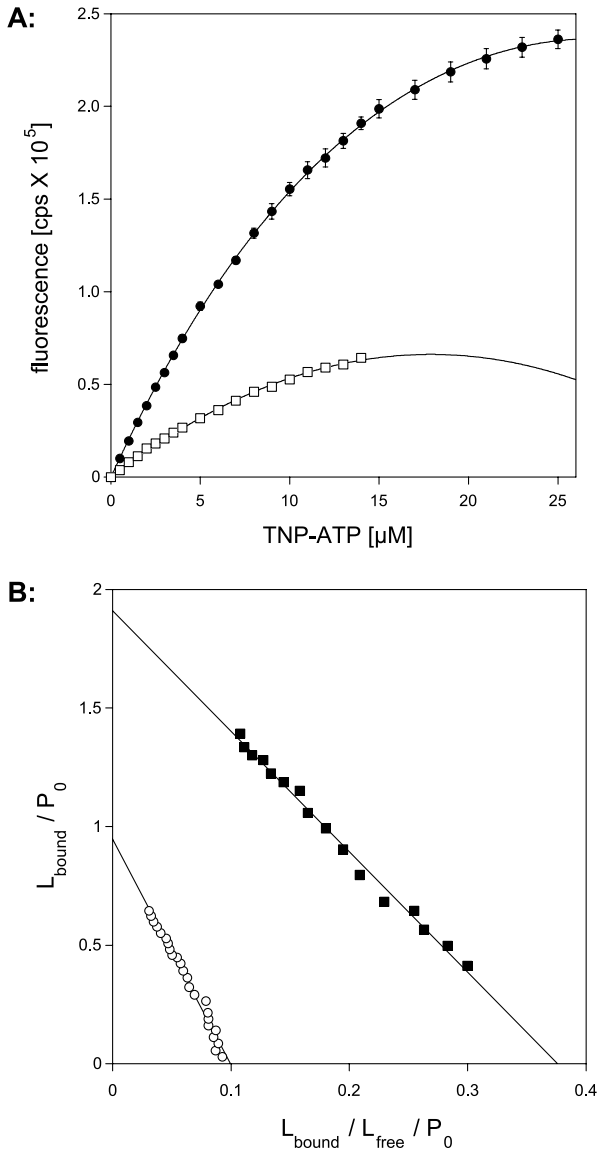

Figure 5. Equilibrium binding of TNP–ATP to OpuAA. (A) TNP–ATP was stepwise added to buffer B supplemented with 150 mM NaCl (□). The fluorescence was followed at 540 nm and analyzed according to equation (7). The same experiment was performed in the presence of 6.2 μM monomeric OpuAA (●) and the fluorescence data were analyzed according to equation (8). (B) Equilibrium binding of TNP–ATP to monomeric (○) or dimeric (■) OpuAA was performed as described in Material and Methods. The fluorescence data were analyzed according to equation (9).

glutamic acid residue, adjacent to the Walker B aspartic acid residue was mutated to a glutamine residue. These mutants showed stable ATP binding, but were either unable to hydrolyze ATP[28] or displayed drastically reduced ATPase activity.[29] Stable formation of a homodimeric mutant MJ0796 (E171Q) or MJ1267 (E179Q) had been observed in the presence of 2 mM ATP (but not in the presence of AMP-PNP), with K_D values of around 70 nM. Interestingly, wild-type MJ0796/ATP complexes could not be detected, although there was no Mg^{2+} to prevent ATP hydrolysis. Supporting these biochemical data, the recently solved structure of MJ0796 (E171Q) in complex with ATP showed a dimer with two ATP molecules bound to the complex. The addition of Mg^{2+} diminished dimer formation of MJ0796 (E171Q),[28] which is in agreement with our data. Possibly, subsequent Mg^{2+} binding to the NBD/ATP complex induces conformational changes, which destabilize the dimer interface of the NBD. The ABC-related protein Rad50 is the only example for a stable dimeric NBD/AMP-PNP/Mg^{2+} complex.[37] The addition of ADP or ADP/Mg^{2+} to OpuAA strongly inhibited dimer formation, and the apparent K_D value was shifted to values of more than 200 μM. Similar observations have been reported for MJ0796, MJ0796 (E171Q),[28] and the NBD of Mdl1p[29] in the presence of ADP. Under these post-hydrolysis conditions, the monomer was the preferred species. In contrast to the data reported here, the NBD of Mdl1p displayed no detectable steady-state ATPase activity in the monomeric state,[29] while the dimeric species was the catalytic active one. Here, both monomer and dimer species displayed basal ATPase activity. Furthermore, no dimeric state was observed for the nucleotide-free state of the Mdl1p-NBD. Dimerization was clearly induced by ATP. However, one has to keep in mind that OpuAA contains a C-terminal extension, which is absent in the Mdl1p-NBD and might play an important role in the dimerization of the nucleotide-free state.

Affinity and stoichiometry of monomeric and dimeric OpuAA/ATP complexes

To understand the effects of nucleotides on M/D equilibrium of OpuAA in more detail, affinity and stoichiometry of TNP–ATP to monomeric or dimeric OpuAA was determined. Competition experiments with ATP or ADP were performed to demonstrate specificity of nucleotide binding and to determine K_D values for OpuAA/ATP or OpuAA/ADP complexes.

As described above, NaCl and $MgCl_2$ have an important influence on M/D interconversion and on the ATPase activity of OpuAA (Figure 2(B), Table 1). Binding of TNP–ATP to OpuAA was, therefore, analyzed at low or high NaCl concentration (150 mM or 1 M, respectively) and in the absence or presence of 5 mM $MgCl_2$. First, TNP–ATP binding to monomeric or dimeric OpuAA in buffer B supplemented with 150 mM NaCl was analyzed. The specific fluorescence constants Q_1 and Q_2 for these assay conditions were calculated as described in Material and Methods (Figure 5(A)). Monomeric or dimeric OpuAA was diluted into assay buffer and immediately titrated with TNP–ATP. Compared to the TNP–ATP fluorescence in the absence of protein, the TNP–ATP fluorescence in the presence of OpuAA was increased several fold, indicating the formation of

Table 2. Dissociation constants and stoichiometry of OpuAA/TNP–ATP complexes at 20(±1) °C determined by equilibrium-binding experiments (see Material and Methods)

Oligomeric species	NaCl (M)	$MgCl_2$	K_D (μM)	Ligand number
Monomer	0.15	–	9.5 ± 0.1	0.95 ± 0.01
Dimer	0.15	–	5.1 ± 0.1	1.91 ± 0.01
Monomer	0.15	+	7.8 ± 0.5	0.96 ± 0.03
Dimer	0.15	+	34 ± 5	2.1 ± 0.3
Monomer	1	+	6.8 ± 0.7	1.01 ± 0.05
Dimer	1	+	22 ± 4	2.1 ± 0.2

an OpuAA/TNP–ATP complex (Figure 5(A)). The fluorescence data for monomeric and dimeric OpuAA were analyzed according to equations (8) and (9) (Figure 5(B)). The K_D values for monomeric and dimeric OpuAA were similar (monomer: 9.5(±0.1) μM; dimer: 5.1(±0.1) μM) (Table 2). The stoichiometry of bound ligands to OpuAA was in agreement with the oligomerization state of the protein (monomer: 0.95 ± 0.01; dimer: 1.91 ± 0.01) (Table 2). These results demonstrated that both monomeric and dimeric OpuAA bound TNP–ATP under the assay conditions. Addition of 5 mM Mg^{2+} did not alter the K_D value and ligand number (N) of monomeric OpuAA complexes significantly (K_D: 7.8(±0.5) μM; N: 0.96 ± 0.03) (Table 2). However, for dimeric OpuAA the K_D value increased to 34(±5) μM (Table 2), suggesting that Mg^{2+} destabilizes a dimeric OpuAA/TNP–ATP complex. TNP–ATP binding to monomeric or dimeric OpuAA in buffer B supplemented with 1 M NaCl and 5 mM Mg^{2+} was also tested. K_D values and stoichiometry of OpuAA/TNP–ATP complexes for these assay conditions are summarized in Table 2.

Competition experiments of OpuAA/TNP–ATP complexes

To demonstrate specificity of TNP–ATP binding to OpuAA, non-labeled adenine nucleotides (ATP or ADP) were added to pre-formed OpuAA/TNP–ATP complexes in a stepwise fashion. These competition experiments were performed at two different salt conditions (150 mM NaCl and 1 M NaCl, respectively) in the absence or presence of $MgCl_2$.

In the first experiments, buffer B was supplemented with 150 mM NaCl. The fluorescence of pre-formed monomeric or dimeric OpuAA/TNP–ATP complexes decreased with increasing concentrations of ATP (Figure 6(A)). This indicated a competition of ATP for the nucleotide-binding pocket of OpuAA. Identical experiments were performed in the absence of OpuAA and used for background subtraction (see Material and Methods). Fluorescence data were subsequently normalized. Using the K_D of OpuAA/TNP–ATP complexes (see Table 2) and the concentration of

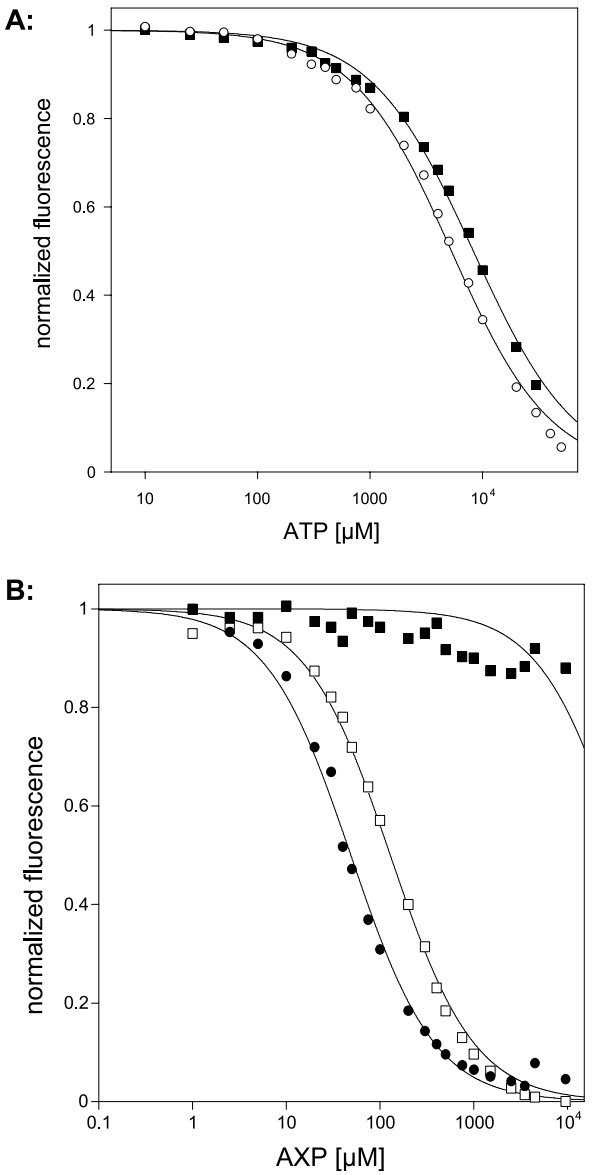

Figure 6. Competition experiments of OpuAA/TNP–ATP complexes. (A) OpuAA monomer (○) and dimer (■) were pre-incubated with TNP–ATP (10 μM) in buffer B supplemented with 150 mM NaCl, and ATP was added stepwise. Normalised fluorescence at 540 nm was analyzed according to equation (10). (B) OpuAA monomer or dimer were pre-incubated with TNP–ATP (10 μM) in buffer B supplemented with 1 M NaCl. AXP was added stepwise and normalised fluorescence was analyzed according to equation (10). Monomer, X = T (□); monomer, X = D (●); dimer, X = T (■).

OpuAA and TNP–ATP, K_D values of OpuAA/ATP complexes were calculated according to equation (10). The K_D was calculated to be 2.8(±0.3) mM for monomeric OpuAA/ATP and 3.5(±0.5) mM for dimeric OpuAA/ATP (Table 3). These results clearly demonstrate that TNP–ATP binding to monomeric or dimeric OpuAA is specific. However, the affinity of OpuAA to ATP is lower than to TNP–ATP, roughly by a factor of

Table 3. Dissociation constants of OpuAA/AXP complexes at 20(±2) °C determined by competition experiments (see Material and Methods)

Oligomeric species	NaCl (M)	$MgCl_2$	Ligand	K_D (mM)
Monomer	0.15	−	ATP	2.8 ± 0.3
Dimer	0.15	−	ATP	3.5 ± 0.5
Monomer	0.15	+	ATP	0.45 ± 0.05
Dimer	0.15	+	ATP	1.8 ± 0.3
Monomer	0.15	+	ADP	0.09 ± 0.01
Monomer	1	+	ATP	0.054 ± 0.004
Dimer	1	+	ATP	> 10
Monomer	1	+	ADP	0.02 ± 0.002

1000. This is in agreement with the reported data of Thoenges *et al*.[55] K_D values of OpuAA/ATP or ADP complexes in the presence of Mg^{2+} are summarized in Table 3.

In the second group of experiments, buffer B was supplemented with 1 M NaCl and 5 mM $MgCl_2$. The experiments were performed as described above using ATP or ADP as competitor for TNP–ATP (Figure 6(B)). After background subtraction and normalization, K_D values were calculated according to equation (10). In case of monomeric OpuAA, K_D values were 54(±4) μM (OpuAA/ATP) and 20(±2) μM (OpuAA/ADP) (Table 3). In case of dimeric OpuAA the fluorescence of OpuAA/TNP–ATP could not be decreased substantially by addition of ATP. This implies a low affinity of ATP to dimeric OpuAA (larger than 10 mM) or a non-exchangeability of TNP–ATP in this functional state. Such non-exchangeability has been described, for example, for the NBD/ATP complex of Mdl1p.[29]

Time-course of fluorescence of OpuAA/TNP–ADP complexes

When a fluorescence titration of dimeric OpuAA with TNP–ADP/Mg^{2+} was performed, the fluorescence signal did not remain constant (as it did with TNP–ATP/Mg^{2+}), but increased over the time. To investigate this in more detail, we diluted monomeric or dimeric OpuAA in buffer B supplemented with 150 mM NaCl and 10 μM TNP–ADP in the absence or presence of 5 mM $MgCl_2$ and monitored the fluorescence over time. One should consider that under these buffer conditions the M/D interconversion of OpuAA was possible. In the absence of $MgCl_2$, addition of monomeric or dimeric OpuAA to assay buffer showed a similar immediate increase in fluorescence (about 4×10^4 cps) and the fluorescence signal remained constant over the whole period of measurement, indicating a stable binding event (Figure 7(c) and (d)). An approximately tenfold immediate increase in fluorescence was detected upon addition of monomeric OpuAA to assay buffer containing 5 mM Mg^{2+}. The fluorescence signal remained constant during the measurement

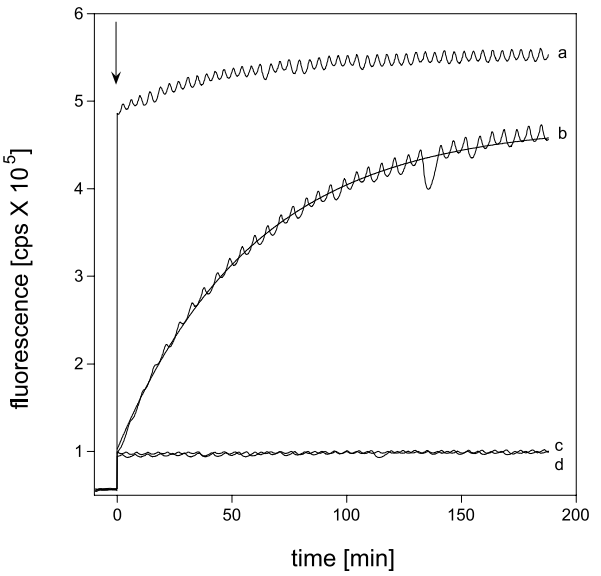

Figure 7. Time-course of TNP–ADP fluorescence at 540 nm of samples containing buffer B supplemented with 150 mM NaCl and 10 μM TNP–ADP. The arrow indicates the time point of addition of 3 μM monomeric (a and c) or 1.5 μM dimeric (b and d) OpuAA. Samples a and b were additionally supplemented with 5 mM $MgCl_2$. Fluorescence was analyzed according to equation (11).

(Figure 7(a)). Addition of dimeric OpuAA to Mg^{2+}-supplemented assay buffer resulted in the same final value of fluorescence (Figure 7(b)). However, fluorescence increased gradually over time, which allowed an analysis of the data according to equation (11). The half-time was determined to be 50(±1) min.

This drastic increase in fluorescence of the OpuAA/TNP–ADP/Mg^{2+} complex (compared to OpuAA/TNP–ADP complexes) was caused by a roughly tenfold higher γ value. In agreement with this observation, γ was determined independently (see Material and Methods) for OpuAA/TNP–ADP/Mg^{2+} complex to be 40. Since the enhancement factor reflects the sensing of the TNP fluorophor to the protein environment within the nucleotide-binding site of OpuAA, this result implies that drastic rearrangements or conformational changes of OpuAA upon binding of TNP–ADP/Mg^{2+} were responsible for the increase in γ. For the maltose transport system the incorporation of ADP/Mg^{2+}/vanadate, as a transition state analogue, caused a shift in the emission wavelength of fluorescently labeled complexes. This shift was associated with a conformational change from the ground state to the transition state of MalK upon activation of ATPase activity.[56] In support of this explanation, partial proteolytic digestion of HlyB-NBD in presence or absence of ADP/Mg^{2+} suggested a nucleotide induced conformational change of HlyB-NBD.[57]

The increase in fluorescence showed a

monoexponential time-course with a half time of 50(±10) min. However, TNP–ADP/Mg^{2+} binding to dimeric OpuAA might be kinetically disfavored. *In vivo*, when OpuAA/ADP/Mg^{2+} complexes are formed immediately as in the post-hydrolysis state of the catalytic cycle, the half-time might be decreased several fold. Furthermore, in the presence of the TMDs, the kinetics might be altered, resulting in an accelerated rate.[58] However, our observation implies that observed thermodynamic pathways are already present in the isolated NBD. In previous experiments it had been demonstrated that ADP/Mg^{2+} caused a decay of dimeric OpuAA and that monomeric OpuAA was the preferred oligomeric species under these conditions. Taken together, these results led to the conclusion that addition of ADP/Mg^{2+}, as a mimic for the post-hydrolysis state of OpuAA within the ATP hydrolysis cycle, induced a conformational change within the dimer interface of OpuAA. This may lead to a decay of dimeric OpuAA due to a loss of affinity within the two OpuAA monomers.

Model of the ATP hydrolysis cycle of OpuAA

The change in oligomerization state of NBDs within the catalytic cycle represents a feasible mechanism for the transfer of the chemical energy of ATP hydrolysis to the TMDs. Especially the formation of an NBD/ATP "sandwich dimer", as described by Smith *et al.*,[32] would enable substrate translocation in a well-coordinated fashion. In addition to the cross-talk of NBDs among each other, the NBDs also interact with their cognate TMDs. The TMDs are dimerized and form the translocation pathway for the substrate. This implies a close proximity of the NBDs at the membrane surface, as observed in the crystal structure of the BtuCD complex.[22]

On the basis of our data we propose a model that couple ATP hydrolysis with a change in oligomeric state of OpuAA (Figure 8). In this study, we observed a dynamic M/D interconversion of isolated OpuAA in the nucleotide-free state. A K_D value of 6 μM was calculated for the M/D equilibrium. We suggest that *in vivo* when OpuAA is interacting with its cognate TMD, dimeric OpuAB, the functional oligomeric species is an NBD dimer. M/D equilibrium might be regulated with a K_D value in the low micromolar range. Another example of subunit interaction at a membrane is the recognition of T-cell receptor and MHC class II molecules.[59] In this case, the K_D value of the subunit complex is also in the low micromolar range and is sufficient to ensure interaction of the components and subsequently trigger signal transduction.

Dimeric OpuAA binds two ATP molecules, as demonstrated by equilibrium-binding experiments with TNP–ATP. This implies that dimeric OpuAA represents a functional state in the catalytic cycle. The dissociation constants of monomeric OpuAA/ATP and dimeric OpuAA/ATP complexes are similar (monomer: 2.8 mM; dimer: 3.5 mM). These data enabled us to calculate a K_D value of 10 μM for the M/D equilibrium of OpuAA in its ATP-bound form according to the principle of microscopic reversibility. This K_D value is 100 times greater than the K_D value of MJ0796 (E171Q) in its ATP-bound form. However, the wild-type MJ0796 does not show any dimer formation in presence of ATP. We propose that ATP binds to the pre-formed dimeric NBDs, which interact with their cognate TMDs. As in case of MJ0796 (E171Q) the addition of Mg^{2+} influenced the M/D equilibrium of OpuAA. The addition of 10 mM AMP-PNP/Mg^{2+} to OpuAA shifted the apparent K_D value from 6(±1) μM to 50(±4) μM. In agreement with the shifted apparent K_D value, the dissociation

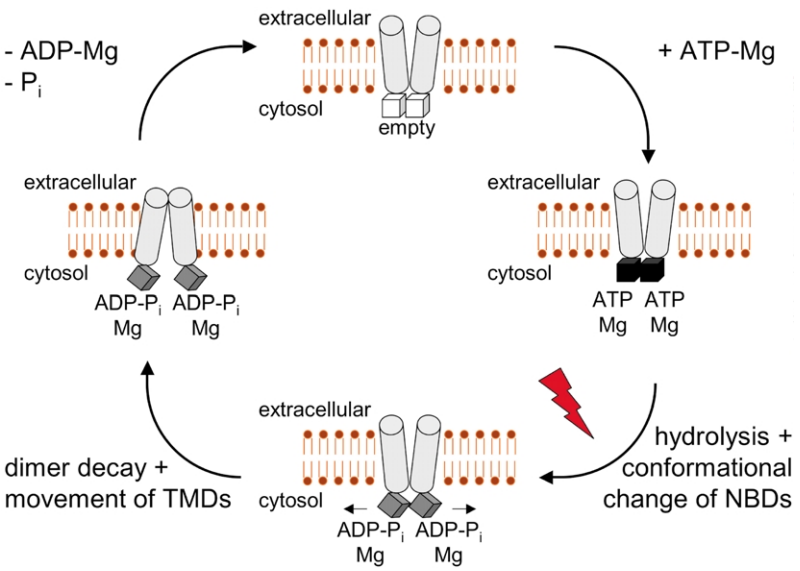

Figure 8. Model of OpuAA hydrolysis cycle. Cubes and barrels depict the NBD (OpuAA) and TMD (OpuAB), respectively. For simplicity, the substrate-binding protein (OpuAC) has been omitted. The flash indicates ATP hydrolysis and subsequent conformational change of OpuAA. Orientation of OpuAB is deduced from the X-ray structure of BtuCD.[22] The movement of the TMDs is of course speculative and only intended to highlight speculative changes occurring within the TMDs upon dissociation of the NBDs, which is used to shuttle the transport substrate.

constants of monomeric OpuAA/ATP/Mg^{2+} and dimeric OpuAA/ATP/Mg^{2+} complexes differ by a factor of almost 3 (monomer: 0.45 mM; dimer: 1.8 mM). If we calculate the dissociation constant of M/D equilibrium of OpuAA in its ATP/Mg^{2+}-bound form according to the principle of microscopic reversibility, a K_D value of 96 μM is derived. This is in agreement with the apparent K_D value for the M/D equilibrium of OpuAA in presence of 10 mM AMP-PNP/Mg^{2+}. We suggest, that the shift in K_D value of M/D equilibrium of OpuAA *in vivo* simply reflects a loss of attractive forces of the two OpuAA monomers within the interface of dimeric OpuAA. This may be a consequence of the rearrangement or conformational change in OpuAA upon binding ATP/Mg^{2+}.

In case of ADP/Mg^{2+} binding to OpuAA, we have clearly detected a conformational change using TNP–ADP as a reporter. The fluorescence of OpuAA/TNP–ADP/Mg^{2+} complexes is enhanced several fold compared to OpuAA/TNP–ADP or OpuAA/TNP–ATP complexes. Changes in the γ value reflect alterations of the protein environment within the nucleotide-binding pocket of OpuAA. Furthermore, the addition of ADP/Mg^{2+} leads to a dissociation of dimeric OpuAA. In agreement with this observation, the apparent K_D value for M/D equilibrium in presence of ADP/Mg^{2+} is greater than 200 μM. As a result, monomeric OpuAA is the preferred oligomeric species under these conditions. We speculate that this dramatic loss of attractive forces for the two monomers within dimeric OpuAA is transmitted to the TMDs, since OpuAA is bound to its cognate TMD $(OpuAB)_2$. The reorganization of the TMDs could then represent the signal on the membrane surface to import the substrate. The release of ADP/Mg^{2+} from OpuAA would then lead to a re-dimerization of nucleotide-free OpuAA and closure of the translocation pathway.

Material and Methods

Cloning of the *opuAA* gene

The *opuAA* gene of *B. subtilis* was amplified by PCR using the *opuA*$^+$ plasmid pBKB1[11] as template. Either 5′ or 3′ extensions encoding a hexahistidine tag as well as 5′ *Nde*I and a 3′ *Hin*dIII restriction sites were introduced using the following combinations of primers. N-His forward: 5′GGAATTCCATATGCATCACCATCACCATCA CAGTGTAGATGAGAAACCAATTAAG3′; N-His reverse: 3′TAGGAAGACGTGTCCTCCACTTTATTATT CGAAATATATA5′ and C-His forward: 5′GGAATTCCA TATGAGTGTAGATGAGAAACCAATTA-3′, C-His reverse: 3′GTTCTAGGAAGACGTGTCCTCCACTTTGT AGTGGTAGTGGTAGTGATTATTCGAAATATATA5′. The PCR products were digested with *Nde*I/*Hin*dIII (NEB, Frankfurt/Main, Germany) and cloned into the L(+)-arabinose-inducible expression vector pBAD33.[60] Both gene inserts were sequenced according to the dideoxynucleotid method and were found to be free of mutations. The *E. coli* strain BL21(DE3) was transformed with the plasmids pBAD33/His_6-OpuAA or pBAD33/OpuAA-His_6.

Overproduction of the OpuAA protein in *E. coli* and its purification

Fifty-millilitre Luria-Bertani media (LB) supplemented with 30 μg/ml chloramphenicol (LB/cam) were inoculated with a single bacterial colony of BL21(DE3) containing either plasmid pBAD33/His_6-OpuAA or pBAD33/OpuAA-His_6. The cultures were incubated overnight on a shaker at 220 rpm and 30 °C. One litre LB/cam medium in a two-litre flask was inoculated with 20 ml of an overnight culture and incubated at 220 rpm and 25 °C. Production of the His_6-tagged OpuAA proteins was induced at an $A_{550\,nm} = 1.5$ with 0.01% (w/v) L(+)-arabinose. After three hours of incubation, the *E. coli* cells were harvested (4000*g*, 15 minutes, 4 °C), resuspended in 15 ml buffer A (50 mM NaP_i, 100 mM NaCl, 10 mM imidazole, pH 8.0), treated with lysozyme (1 mg/ml in buffer A) for 30 minutes at 4 °C and lysed by ultra sonication. The cytosolic protein fraction was isolated by high-speed centrifugation (37,000*g*, 30 minutes, 4 °C) and the supernatant was loaded onto a Zn^{2+}/IDA column (5 ml bed volume, Pharmacia, Freiburg, Germany). Unspecific bound proteins were eluted with 15 column volumes of buffer A and subsequently a linear imidazole gradient (10–300 mM in buffer A) was applied. Recombinant His_6-OpuAA or OpuAA-His_6 was eluted around 200 mM imidazole. The OpuAA-containing fractions were pooled and analyzed by SDS-PAGE, concentrated with an Amicon concentration cell (Millipore, Eschborn, Germany; 10 kDa MWCO) to the appropriate volume and applied onto a Superdex 200 HR column (320 ml bed volume, Pharmacia, Freiburg, Germany) to separate aggregates from the soluble OpuAA protein. Fractions containing OpuAA M/D were pooled and stored at 4 °C until further use at a concentration of approximately 1 mg/ml.

Determination of protein concentration

Protein concentration was determined spectroscopically at 280 nm. The theoretical extinction coefficient ε of monomeric OpuAA was calculated using the expasy server† to be 11,520 $M^{-1}\,cm^{-1}$. Alternatively, protein concentration was determined by the bicinchoninic acid assay (Interchim, Monluçon Cedex, France) according to the protocol of the manufacturer. Total OpuAA concentration always referred to monomeric OpuAA.

Determination of OpuAA M/D ratio

The M/D ratio of OpuAA was analyzed by SEC. Protein solution (1–30 μM), 100–500 μl was loaded onto a Superdex 200 HR column (24 ml bed volume, Pharmacia, Freiburg, Germany) equilibrated in buffer B (10 mM NaP_i, 0.1 mM EDTA, pH 7.5) supplemented with 1 M NaCl. For molecular weight (MW) determination, the column was calibrated using the following proteins: carboanhydrase (29 kDa), bovine serum albumin (66 kDa), alcohol dehydrogenase (150 kDa), amylase (200 kDa) and apoferritin (440 kDa) dissolved in buffer B supplemented with 1 M NaCl. High ionic

† http://www.expasy.ch

strength was chosen to freeze the dynamic M/D equilibrium of OpuAA in order to avoid dilution-dependent changes in the M/D ratio (see Results and Discussion). Protein elution was monitored at 216 nm and the M/D ratio was calculated according to equation (1):

$$\frac{[M]}{c_0} = \frac{A_{216,monomer}}{A_{216,dimer} + A_{216,monomer}}, \qquad \frac{[D]}{c_0} = \frac{1}{2}\left(1 - \frac{[M]}{c_0}\right) \tag{1}$$

Here, $A_{216,monomer}$ and $A_{216,dimer}$ correspond to the maximum absorbance of monomeric and dimeric OpuAA at 216 nm. c_0, [M] and [D] are the concentration of total, monomeric and dimeric OpuAA, respectively.

Kinetic and thermodynamic evaluation of M/D ratio

The K_D of the M/D equilibrium was calculated by the law of mass action according to equation (2):

$$\frac{[M]}{c_0} = \frac{1}{c_0}\left(-\frac{K_D}{4} + \sqrt{\frac{K_D^2}{16} + \frac{c_0 K_D}{2}}\right) \tag{2}$$

Here, c_0 and [M] denote the concentration of total and monomeric OpuAA, respectively. K_D is the dissociation constant.

The time-dependent decay of dimeric OpuAA at 150 mM NaCl and 1 M NaCl was analyzed according to equations (3a) and (3b), respectively (see Supplementary Material):

$$\frac{[D]_{,t}}{c_0} = \frac{k_2 \operatorname{arccot}\left(-\frac{1}{2}(t + k_1)k_2\right)}{8k_{off}c_0} + \frac{K_D}{8c_0} + \frac{1}{4} \tag{3a}$$

$$\frac{[D]_{,t}}{c_0} = \frac{[D]_{,t=0}}{c_0} e^{-t/\tau} \tag{3b}$$

Here, c_0 and [D] denote the concentration of total and dimeric OpuAA, respectively. K_D and k_{off} are the dissociation constant and the off rate of M/D equilibrium, respectively. t and τ denote the time of sample incubation and the half-time of the decay, respectively. k_1 and k_2 are fitting parameters.

ATPase activity assay

ATPase activity of OpuAA was analyzed by a pyruvate kinase/lactate dehydrogenase (PK/LDH) enzyme assay, which uses NADH oxidation to regenerate consumed ATP. The decrease in NADH concentration as a direct measure for ATP consumption was followed spectroscopically at 340 nm with an ELISA reader (GMB Labtechnologies, Jena, Germany) in a 96-well plate (Greiner, Kremsmünster, Germany). The assay was calibrated with different NADH concentrations to give a molar extinction coefficient of NADH of 2590 M^{-1}.

To each well, 0.2 mM NADH, 1.5 mM phosphoenolpyruvate, 45 mM Tris–HCl (pH 8.0), 5 mM $MgCl_2$, five units PK, seven units LDH and 50 µl OpuAA (in buffer B supplemented with the appropriate salt; final concentration 5–10 µM) were added. ATP was added from a Na_2ATP stock solution, pH 6.8. After selecting the desired salt concentration, the final volume of each assay was adjusted with water to 200 µl. After two minutes of incubation, absorbance at 340 nm was monitored at one-minute time intervals over a period of 15 minutes at 22(±2) °C. Data points of the whole measuring period or until all NADH was consumed (at least over a period of seven minutes) were used to calculate linear slopes $\Delta A/\Delta t_{OpuAA}$. To account for ATP autohydrolysis, identical assays were performed in the absence of OpuAA. After background subtraction ($\Delta\Delta A/\Delta\Delta t = (\Delta A/\Delta t_{OpuAA}) - (\Delta A/\Delta t_{buffer})$) reaction velocities were calculated according to equation (4):

$$v = \frac{\Delta\Delta A}{\Delta\Delta t}\frac{1}{2590\ M^{-1}c_0} \tag{4}$$

Here, v is the reaction velocity, $\Delta\Delta A/\Delta\Delta t$ denote the linear slopes of the time dependent decay of NADH absorbance at 340 nm of OpuAA samples after background subtraction and c_0 is the final concentration of OpuAA.

Reaction velocities represent the average value of two independent measurements. Reaction velocities at different ATP concentrations were analyzed according to equation (5) to determine the individual kinetic parameters:

$$v = \frac{[ATP]k_2}{[ATP] + K_M} \tag{5}$$

Here, v is the reaction velocity. K_M and k_2 denote the Michaelis–Menten constant and the turnover number, respectively.

TNP–ATP-binding studies

To assess the binding affinity and stoichiometry of ATP to OpuAA, we used the fluorescent ATP analogue TNP–ATP (2′,3′-*O* (2,4,6-trinitrophenylcyclo-hexadienylidene)-adenosine triphoshate (Molecular Probes, Leiden, Netherlands)). Binding studies were generally performed as described.[61,62] Fluorescence of the TNP nucleotides was monitored at 540 nm using a Fluorolog, (Horiba, Edison, NJ, USA). The excitation wavelength was set at 409 nm, the slit width at 4 nm; temperature was maintained at 20(±1) °C by a circulating water bath. For all experiments, buffer B supplemented with the appropriate salt and $MgCl_2$ was used as assay buffer.

Typically, a 15-nm blue shift of the maximum emission wavelength from 550 nm to 535 nm was observed after binding of TNP–ATP or TNP–ADP/Mg^{2+} to OpuAA. Furthermore, fluorescence intensity was enhanced several-fold. The absolute magnitude depends on the specific protein environment within the nucleotide-binding pocket. The fluorescent enhancement factor (γ) is the ratio of fluorescence intensity at infinite protein concentration with all dye bound (F_{max}) to buffer alone at a fixed TNP–ATP concentration ($\gamma = F_{max}/F_{buffer}$). γ was independently determined by measuring fluorescence intensity with increasing OpuAA concentrations at 4 µM TNP–ATP. F_{max} was determined by fitting the data with a single exponential equation (equation (6)). γ was calculated to be 5.7 ± 0.3 in buffer B supplemented with 150 mM NaCl and 3.0 ± 0.2 in buffer B supplemented with 1 M NaCl and 5 mM $MgCl_2$:

$$F_{total} = F_{buffer} + F_{max}(1 - e^{-k_2 c_0}) \tag{6}$$

Here, F_{total} and F_{buffer} are the measured fluorescence in the presence or absence of OpuAA. c_0 denotes the concentration of OpuAA. F_{max} and k_2 are specific fitting parameters.

Fluorescence intensity of TNP–ATP in buffer is low in the absence of OpuAA and can be described by equation (7), taking inner filter effects into account. The

fluorescence constants Q_1 and Q_2 were determined by stepwise addition of TNP–ATP (0.5 μM steps for 0–4 μM and 1.0 μM steps for 4–14 μM) from a 1 mM stock solution to assay buffer. Maximal dilution was below 1% (v/v). Fluorescence was measured 30 seconds after addition and mixing to allow for equilibration. All data were corrected for fluorescence in the absence of TNP–ATP and were averaged by at least two independent measurements. Q_1 and Q_2 were calculated to be $7403(\pm 85)\ \mu M^{-1}$ and $-207(\pm 8)\ \mu M^{-2}$, respectively, in buffer B supplemented with 150 mM NaCl. Q_1 and Q_2 were calculated to be $6429(\pm 51)\ \mu M^{-1}$ and $-148(\pm 4)\ \mu M^{-2}$, respectively, in buffer B supplemented with 1 M NaCl and 5 mM $MgCl_2$:

$$F_{\text{buffer}} = Q_1 L_0 + Q_2 L_0^2 \tag{7}$$

Here, Q_1 and Q_2 denote the specific fluorescence constants of TNP–ATP and L_0 is the concentration of TNP–ATP.

Protein was diluted into buffer B supplemented with NaCl (final protein concentration 3–6 μM) and titrated immediately as described above or even to higher TNP–ATP concentrations. The dissociation constant (K_{D_L}) and the corresponding ligand number (N) of OpuAA/TNP–ATP complexes were determined according to equation (8). For explicit derivation of equation (8) see Supplementary Material:

$$F_{\text{total}} = Q_1 L_0 + Q_2 L_0^2 + \left((\gamma - 1)\frac{Q_1}{2} - L_0 Q_2\right) \times [A - \sqrt{A^2 - 4L_0 N P_0}] \tag{8}$$

$$A = (K_{D_L} + L_0 + N P_0)$$

Here, Q_1 and Q_2 denote specific fluorescence constants and γ is the enhancement factor. K_{D_L} and N are the dissociation constant and the ligand number of OpuAA/TNP–ATP complexes, respectively. L_0 and P_0 are the total concentration of TNP–ATP and OpuAA, respectively. OpuAA concentrations were calculated taking the oligomerization status of the protein into account. F_{total} defines the measured fluorescence.

For alternative analysis of the equilibrium-binding fluorescence data, we applied a Scatchard analysis according to equation (9):

$$\frac{L_{\text{bound}}}{P_0} = N - K_{D_L}\frac{L_{\text{bound}}}{L_{\text{free}} P_0} \tag{9}$$

Here, L_{bound} and L_{free} denote concentration of bound and free TNP–ATP, respectively (see equations (IV) and (Ia) in the Supplementary Material). K_{D_L} and N are the dissociation constant and the corresponding ligand number of OpuAA/TNP–ATP complexes, respectively. P_0 is the total concentration of monomeric or dimeric OpuAA, taking the oligomerization status of the protein into account.

Competitive binding studies of OpuAA/TNP–ATP complexes

OpuAA (2–4 μM) were pre-incubated with 10 μM TNP–ATP for five minutes at 20(±2) °C. Subsequently, AXP (X = T or D) was added in a stepwise fashion from a 1, 10, 100 or 500 mM stock solution at pH 6.8 to a final ATP concentration of maximal 50 mM. Maximal dilution was less than 5% (v/v). Identical experiments were performed in the absence of OpuAA. Fluorescence data in the presence and absence of OpuAA were subtracted and analyzed according to equation (10). For explicit derivation of equation (10) see Supplementary Material:

$$\frac{F_{\text{PL}_N,\text{AXP}\neq 0}}{F_{\text{PL}_N,\text{AXP}=0}} = \frac{A + \text{AXP}_0\frac{K_{D_L}}{K_{D_{AXP}}} - \sqrt{\left(A + \text{AXP}_0\frac{K_{D_L}}{K_{D_{AXP}}}\right)^2 - 4NP_0L_0}}{A - \sqrt{A^2 - 4NP_0L_0}} \tag{10}$$

$$A = (K_{D_L} + L_0 + NP_0)$$

Here, $F_{\text{PL}_{N,\text{AXP}\neq 0}}/F_{\text{PL}_{N,\text{AXP}=0}}$ defines the normalized fluorescence at different AXP concentrations (AXP_0, X = T, D). K_{D_L} and N are the dissociation constant and the corresponding ligand number of OpuAA/TNP–ATP complexes, respectively. L_0 and P_0 are the total concentrations of TNP–ATP and OpuAA, respectively. OpuAA concentrations were calculated taking the oligomerization status of the protein into account. $K_{D_{AXP}}$ is the dissociation constant of OpuAA/AXP complexes.

K_D values of OpuAA/AXP complexes are the average value of at least two independent titration experiments.

Time-course of TNP–ADP fluorescence

Monomeric (3 μM) or dimeric (1.5 μM) OpuAA were added at the indicated time to buffer B supplemented with 150 mM NaCl and 10 μM TNP–ADP (2′,3′-*O* (2,4,6-trinitrophenylcyclo-hexadienylidene)-adenosine diphosphate, (Molecular Probes, Leiden, Netherlands)) in the absence or presence of 5 mM $MgCl_2$. The fluorescence at 540 nm was monitored at ten-second time points over a period of 200 minutes at 20(±2) °C. The time-dependent increase in fluorescence was analyzed according to equation (11):

$$F_{\text{total}} = k_1 + k_2(1 - e^{-t/\tau}) \tag{11}$$

Here, k_1 and k_2 are constants. t and τ denote time of fluorescence measurement and half-time of fluorescence increase, respectively. F_{total} is the measured fluorescence at 540 nm.

All chemicals were purchased from Sigma, Taufkirchen, Germany unless otherwise indicated.

Acknowledgements

We thank Robert Tampé, Jacob Piehler and the members of the Institute of Biochemistry for constant encouragement, assistance and stimulating discussions. We are indebted to Jelena Zaitseva & Vickie Bremer for critical reading of the manuscript. This work was supported by the priority program "Struktur funktioneller Module von energiewandelnden Systemen in Prokaryoten" (BR 796/5-1 to E.B.; Schm1279/4-1 to L.S.) of the DFG, the Max-Planck Institute for Terrrestrial Microbiology (Marburg) (to E.B.), by the Fonds der Chemischen Industrie (to E.B.) and the Emmy Noether program of the DFG (grant Schm1279/2-2 to L.S.).

References

1. Kempf, B. & Bremer, E. (1998). Uptake and synthesis of compatible solutes as microbial stress responses to high-osmolality environments. *Arch. Microbiol.* **170**, 319–330.
2. Wood, J. M., Bremer, E., Csonka, L. N., Kraemer, R., Poolman, B., van der Heide, T. & Smith, L. T. (2001). Osmosensing and osmoregulatory compatible solute accumulation by bacteria. *Comp. Biochem. Physiol. A Mol. Integr. Physiol.* **130**, 437–460.
3. Galinski, E. A. (1995). Osmoadaptation in bacteria. *Advan. Microb. Physiol.* **37**, 272–328.
4. Record, M. T., Jr, Courtenay, E. S., Cayley, S. & Guttman, H. J. (1998). Biophysical compensation mechanisms buffering *E. coli* protein–nucleic acid interactions against changing environments. *Trends Biochem. Sci.* **23**, 190–194.
5. Record, M. T., Jr, Courtenay, E. S., Cayley, D. S. & Guttman, H. J. (1998). Responses of *E. coli* to osmotic stress: large changes in amounts of cytoplasmic solutes and water. *Trends Biochem. Sci.* **23**, 143–148.
6. Whatmore, A. M. & Reed, R. H. (1990). Determination of turgor pressure in *Bacillus subtilis*: a possible role for K+ in turgor regulation. *J. Gen. Microbiol.* **136**, 2521–2526.
7. McLaggan, D., Naprstek, J., Buurman, E. T. & Epstein, W. (1994). Interdependence of K+ and glutamate accumulation during osmotic adaptation of *Escherichia coli*. *J. Biol. Chem.* **269**, 1911–1917.
8. Yan, D., Ikeda, T. P., Shauger, A. E. & Kustu, S. (1996). Glutamate is required to maintain the steady-state potassium pool in *Salmonella typhimurium*. *Proc. Natl Acad. Sci. USA*, **93**, 6527–6531.
9. Brown, A. D. (1976). Microbial water stress. *Bacteriol. Rev.* **40**, 803–846.
10. Kappes, R. M., Kempf, B. & Bremer, E. (1996). Three transport systems for the osmoprotectant glycine betaine operate in *Bacillus subtilis*: characterization of OpuD. *J. Bacteriol.* **178**, 5071–5079.
11. Kempf, B. & Bremer, E. (1995). OpuA, an osmotically regulated binding protein-dependent transport system for the osmoprotectant glycine betaine in *Bacillus subtilis*. *J. Biol. Chem.* **270**, 16701–16713.
12. Kappes, R. M., Kempf, B., Kneip, S., Boch, J., Gade, J., Meier-Wagner, J. & Bremer, E. (1999). Two evolutionarily closely related ABC transporters mediate the uptake of choline for synthesis of the osmoprotectant glycine betaine in *Bacillus subtilis*. *Mol. Microbiol.* **32**, 203–216.
13. Kempf, B., Gade, J. & Bremer, E. (1997). Lipoprotein from the osmoregulated ABC transport system OpuA of *Bacillus subtilis*: purification of the glycine betaine binding protein and characterization of a functional lipidless mutant. *J. Bacteriol.* **179**, 6213–6220.
14. Holland, I. B. & Blight, M. A. (1999). ABC-ATPases, adaptable energy generators fuelling transmembrane movement of a variety of molecules in organisms from bacteria to humans. *J. Mol. Biol.* **293**, 381–399.
15. Higgins, C. F. (2001). ABC transporters: physiology, structure and mechanism—an overview. *Res. Microbiol.* **152**, 205–210.
16. Gottesman, M. M. & Ambudkar, S. V. (2001). Overview: ABC transporters and human disease. *J. Bioenerg. Biomembr.* **33**, 453–458.
17. Gottesman, M. M., Pastan, I. & Ambudkar, S. V. (1996). P-glycoprotein and multidrug resistance. *Curr. Opin. Genet. Dev.* **6**, 610–617.
18. Riordan, J. R., Rommens, J. M., Kerem, B., Alon, N., Rozmahel, R., Grzelczak, Z. *et al.* (1989). Identification of the cystic fibrosis gene: cloning and characterization of complementary DNA. *Science*, **245**, 1066–1073.
19. Schmitt, L. & Tampe, R. (2002). Structure and mechanism of ABC transporters. *Curr. Opin. Struct. Biol.* **12**, 754–760.
20. Ames, G. F., Mimura, C. S., Holbrook, S. R. & Shyamala, V. (1992). Traffic ATPases: a superfamily of transport proteins operating from *Escherichia coli* to humans. *Advan. Enzymol. Relat. Areas Mol. Biol.* **65**, 1–47.
21. Higgins, C. F., Haag, P. D., Nikaido, K., Ardeshir, F., Garcia, G. & Ames, G. F. (1982). Complete nucleotide sequence and identification of membrane components of the histidine transport operon of *S. typhimurium*. *Nature*, **298**, 723–727.
22. Locher, K. P., Lee, A. T. & Rees, D. C. (2002). The *E. coli* BtuCD structure: a framework for ABC transporter architecture and mechanism. *Science*, **296**, 1091–1098.
23. Chang, G. & Roth, C. B. (2001). Structure of MsbA from *E. coli*: a homolog of the multidrug resistance ATP binding cassette (ABC) transporters. *Science*, **293**, 1793–1800.
24. Benabdelhak, H., Kiontke, S., Horn, C., Ernst, R., Blight, M. A., Holland, I. B. & Schmitt, L. (2003). A specific interaction between the NBD of the ABC-transporter HlyB and a C-terminal fragment of its transport substrate haemolysin A. *J. Mol. Biol.* **327**, 1169–1179.
25. Walker, J. E., Saraste, M., Runswick, M. J. & Gay, N. J. (1982). Distantly related sequences in the alpha- and beta-subunits of ATP synthase, myosin, kinases and other ATP-requiring enzymes and a common nucleotide binding fold. *EMBO J.* **1**, 945–951.
26. Hung, L. W., Wang, I. X., Nikaido, K., Liu, P. Q., Ames, G. F. & Kim, S. H. (1998). Crystal structure of the ATP-binding subunit of an ABC transporter. *Nature*, **396**, 703–707.
27. Nikaido, K., Liu, P. Q. & Ames, G. F. (1997). Purification and characterization of HisP, the ATP-binding subunit of a traffic ATPase (ABC transporter), the histidine permease of *Salmonella typhimurium*. Solubility, dimerization, and ATPase activity. *J. Biol. Chem.* **272**, 27745–27752.
28. Moody, J. E., Millen, L., Binns, D., Hunt, J. F. & Thomas, P. J. (2002). Cooperative, ATP-dependent association of the nucleotide binding cassettes during the catalytic cycle of ATP-binding cassette transporters. *J. Biol. Chem.* **277**, 21111–21114.
29. Janas, E., Hofacker, M., Chen, M., Gompf, S., Van Der Does, C. & Tampe, R. (2003). The ATP hydrolysis cycle of the nucleotide-binding domain of the mitochondrial ABC transporter Mdl1p. *J. Biol. Chem.* **278**, 26862–26869.
30. Diederichs, K., Diez, J., Greller, G., Muller, C., Breed, J., Schnell, C. *et al.* (2000). Crystal structure of MalK, the ATPase subunit of the trehalose/maltose ABC transporter of the archaeon *Thermococcus litoralis*. *EMBO J.* **19**, 5951–5961.
31. Yuan, Y. R., Blecker, S., Martsinkevich, O., Millen, L., Thomas, P. J. & Hunt, J. F. (2001). The crystal structure of the MJ0796 ATP-binding cassette. Implications for the structural consequences of ATP hydrolysis in the active site of an ABC transporter. *J. Biol. Chem.* **276**, 32313–32321.
32. Smith, P. C., Karpowich, N., Millen, L., Moody, J. E.,

Rosen, J., Thomas, P. J. & Hunt, J. F. (2002). ATP binding to the motor domain from an ABC transporter drives formation of a nucleotide sandwich dimer. *Mol. Cell*, **10**, 139–149.
33. Karpowich, N., Martsinkevich, O., Millen, L., Yuan, Y. R., Dai, P. L., MacVey, K. *et al.* (2001). Crystal structures of the MJ1267 ATP binding cassette reveal an induced-fit effect at the ATPase active site of an ABC transporter. *Structure*, **9**, 571–586.
34. Gaudet, R. & Wiley, D. C. (2001). Structure of the ABC ATPase domain of human TAP1, the transporter associated with antigen processing. *EMBO J.* **20**, 4964–4972.
35. Schmitt, L., Benabdelhak, H., Blight, M. A., Holland, I. B. & Stubbs, M. T. (2003). Crystal structure of the nucleotide binding domain of the ABC-transporter haemolysin B: identification of a variable region within ABC helical domains. *J. Mol. Biol.* **330**, 333–342.
36. Verdon, G., Albers, S. V., Dijkstra, B. W., Driessen, A. J. & Thunnissen, A. M. (2003). Crystal structures of the ATPase subunit of the glucose ABC transporter from *Sulfolobus solfataricus*: nucleotide-free and nucleotide-bound conformations. *J. Mol. Biol.* **330**, 343–358.
37. Hopfner, K. P., Karcher, A., Shin, D. S., Craig, L., Arthur, L. M., Carney, J. P. & Tainer, J. A. (2000). Structural biology of Rad50 ATPase: ATP-driven conformational control in DNA double-strand break repair and the ABC-ATPase superfamily. *Cell*, **101**, 789–800.
38. Zhou, T., Radaev, S., Rosen, B. P. & Gatti, D. L. (2000). Structure of the ArsA ATPase: the catalytic subunit of a heavy metal resistance pump. *EMBO J.* **19**, 4838–4845.
39. van der Heide, T. & Poolman, B. (2000). Osmoregulated ABC-transport system of *Lactococcus lactis* senses water stress *via* changes in the physical state of the membrane. *Proc. Natl Acad. Sci. USA*, **97**, 7102–7106.
40. van der Heide, T. & Poolman, B. (2000). Glycine betaine transport in *Lactococcus lactis* is osmotically regulated at the level of expression and translocation activity. *J. Bacteriol.* **182**, 203–206.
41. Haardt, M., Kempf, B., Faatz, E. & Bremer, E. (1995). The osmoprotectant proline betaine is a major substrate for the binding-protein-dependent transport system ProU of *Escherichia coli* K-12. *Mol. Gen. Genet.* **246**, 783–786.
42. Panagiotidis, C. H., Boos, W. & Shuman, H. A. (1998). The ATP-binding cassette subunit of the maltose transporter MalK antagonizes MalT, the activator of the *Escherichia coli* mal regulon. *Mol. Microbiol.* **30**, 535–546.
43. Kuhnau, S., Reyes, M., Sievertsen, A., Shuman, H. A. & Boos, W. (1991). The activities of the *Escherichia coli* MalK protein in maltose transport, regulation, and inducer exclusion can be separated by mutations. *J. Bacteriol.* **173**, 2180–2186.
44. Greller, G., Horlacher, R., DiRuggiero, J. & Boos, W. (1999). Molecular and biochemical analysis of MalK, the ATP-hydrolyzing subunit of the trehalose/maltose transport system of the hyperthermophilic archaeon *Thermococcus litoralis*. *J. Biol. Chem.* **274**, 20259–20264.
45. Morbach, S., Tebbe, S. & Schneider, E. (1993). The ATP-binding cassette (ABC) transporter for maltose/maltodextrins of *Salmonella typhimurium*. Characterization of the ATPase activity associated with the purified MalK subunit. *J. Biol. Chem.* **268**, 18617–18621.
46. Davidson, A. L. & Nikaido, H. (1990). Overproduction, solubilization, and reconstitution of the maltose transport system from *Escherichia coli*. *J. Biol. Chem.* **265**, 4254–4260.
47. Fersht, A. (1997). *Enzyme Structure and Mechanism*, W. H. Freeman and Company, San Francisco, CA.
48. van der Heide, T., Stuart, M. C. & Poolman, B. (2001). On the osmotic signal and osmosensing mechanism of an ABC transport system for glycine betaine. *EMBO J.* **20**, 7022–7032.
49. Poolman, B., Blount, P., Folgering, J. H., Friesen, R. H., Moe, P. C. & van der Heide, T. (2002). How do membrane proteins sense water stress? *Mol. Microbiol.* **44**, 889–902.
50. Racher, K. I., Culham, D. E. & Wood, J. M. (2001). Requirements for osmosensing and osmotic activation of transporter ProP from *Escherichia coli*. *Biochemistry*, **40**, 7324–7333.
51. Peter, H., Burkovski, A. & Kramer, R. (1998). Osmo-sensing by N- and C-terminal extensions of the glycine betaine uptake system BetP of *Corynebacterium glutamicum*. *J. Biol. Chem.* **273**, 2567–2574.
52. Rubenhagen, R., Morbach, S. & Kramer, R. (2001). The osmoreactive betaine carrier BetP from *Corynebacterium glutamicum* is a sensor for cytoplasmic K+. *EMBO J.* **20**, 5412–5420.
53. Jung, K., Veen, M. & Altendorf, K. (2000). K+ and ionic strength directly influence the autophosphorylation activity of the putative turgor sensor KdpD of *Escherichia coli*. *J. Biol. Chem.* **275**, 40142–40147.
54. Kennedy, K. A. & Traxler, B. (1999). MalK forms a dimer independent of its assembly into the MalFGK2 ATP-binding cassette transporter of *Escherichia coli*. *J. Biol. Chem.* **274**, 6259–6264.
55. Thoenges, D., Amler, E., Eckert, T. & Schoner, W. (1999). Tight binding of bulky fluorescent derivatives of adenosine to the low affinity E2ATP site leads to inhibition of Na+/K+-ATPase. Analysis of structural requirements of fluorescent ATP derivatives with a Koshland–Nemethy–Filmer model of two interacting ATP sites. *J. Biol. Chem.* **274**, 1971–1978.
56. Mannering, D. E., Sharma, S. & Davidson, A. L. (2001). Demonstration of conformational changes associated with activation of the maltose transport complex. *J. Biol. Chem.* **276**, 12362–12368.
57. Koronakis, V., Hughes, C. & Koronakis, E. (1993). ATPase activity and ATP/ADP-induced conformational change in the soluble domain of the bacterial protein translocator HlyB. *Mol. Microbiol.* **8**, 1163–1175.
58. Axelrod, D. & Wang, M. D. (1994). Reduction-of-dimensionality kinetics at reaction-limited cell surface receptors. *Biophys. J.* **66**, 588–600.
59. Matsui, K., Boniface, J. J., Reay, P. A., Schild, H., Fazekas de St Groth, B. & Davis, M. M. (1991). Low affinity interaction of peptide–MHC complexes with T cell receptors. *Science*, **254**, 1788–1791.
60. Guzman, L. M., Belin, D., Carson, M. J. & Beckwith, J. (1995). Tight regulation, modulation, and high-level expression by vectors containing the arabinose pBAD promoter. *J. Bacteriol.* **177**, 4121–4130.
61. Faller, L. D. (1989). Competitive binding of ATP and the fluorescent substrate analogue 2′,3′-*O*-(2,4,6-trinitrophenylcyclohexadienylidine) adenosine

5′-triphosphate to the gastric H + ,K + -ATPase: evidence for two classes of nucleotide sites. *Biochemistry*, **28**, 6771–6778.
62. Faller, L. D. (1990). Binding of the fluorescent substrate analogue 2′,3′-*O*-(2,4,6-trinitrophenylcyclohexadienylidene)adenosine 5′-triphosphate to the gastric H + ,K(+)-ATPase: evidence for cofactor-induced conformational changes in the enzyme. *Biochemistry*, **29**, 3179–3186.

Edited by I. B. Holland

(Received 23 May 2003; received in revised form 18 September 2003; accepted 21 September 2003)

Supplementary Material for this paper is available on Science Direct